Nonlinear Finite Element Analysis of Composite Shell Under Impact

Chongdu Cho*, Guiping Zhao, Chang Boo Kim
School of Mechanical, Aerospace, and Automation Engineering Inha University

Large deflection dynamic responses of laminated composite cylindrical shells under impact are analyzed by the geometrically nonlinear finite element method based on a generalized Sander's shell theory with the first order transverse shear deformation and the von-Karman large deflection assumption. A modified indentation law with inelastic indentation is employed for the contact force. The nonlinear finite element equations of motion of shell and an impactor along with the contact laws are solved numerically using Newmark's time marching integration scheme in conjunction with Akay type successive iteration in each step. The ply failure region of the laminated shell is estimated using the Tsai-Wu quadratic interaction criteria. Numerical results, including the contact force histories, deflections and strains are presented and compared with the ones by linear analysis. The effect of the radius of curvature on the composite shell behaviors is investigated and discussed.

Key Words : Composite Shell, Impact, Non-Linear Finite Element Analysis, Damage

1. Introduction

Composite laminates are notorious for impact damage. The impact problem of composite laminated plates has been studied extensively in the past decade (Shivakumar, Elber, and Illg, 1985; Aggour and Sun, 1988; Choi and Hong, 1994; Wu and Yen, 1994). In practical applications, most of the composite laminates are not generally flat; but curved in geometry with the increased applications in aerospace, automobile, and petrochemical industries. However, there are relatively few investigations that studied damage as well as the dynamic response of a composite thin shell subjected to impact load. Recently, Matemilola and Stronge (1997) reported an analytical solution for the impact response of a simply supported anisotropic composite cylinder. Gong, Toh, and Shim (1994) proposed a spring-mass model to estimate the contact force of an open curved shell under impact; they expressed a contact force as a function of the material properties and the mass of impactor and laminated shell as well as the initial velocity of the impactor. Bachrach and Hansen (1988) developed a mixed finite element method for a composite cylinder subjected to impact. The displacements of a projectile and cylinder are approximated using the Wilson-method and the finite difference method, respectively, to solve the non-linear equations arising from contact effects. Cho and Zhao (1999) investigated the dynamic response and damage of a composite shell under low velocity impact. However, all of the works cited above are based on the small-deformation theory. This theory is valid for assumed displacements much smaller than the thickness of the shell. However, when the impact velocity becomes relatively large such that the displacements at the impact point are of the order of the shell thickness, the small-deformation theory is not adequate and a large-deflection assumption has to be imposed.

In this paper, the large deflection dynamic

* Corresponding Author,
E-mail : cdcho@dragon.inha.ac.kr
TEL : +82-32-860-7321 ; **FAX** : +82-32-868-1716
School of Mechanical, Aerospace, and Automation Engineering Inha University, 253 Yong Hyun, Nam Ku, Inchon, 402-751 Korea. (Manuscript **Received** December 21, 1999; **Revise** March 7, 2000)

responses of laminated composite cylindrical shells under impact are investigated using the geometrical nonlinear finite element method. A nine-node iso-parametric quadrilateral element based on the Sander's shell theory and the von Karman large deflection assumption is developed for the shell; and the first order transverse shear deformation is considered. In order to calculate the contact force during impact, a modified indentation law (Tan and Sun, 1985) that takes into account the effect of permanent indentation is adapted to a finite element program. The nonlinear finite element equations are solved using the Newmark constant acceleration algorithm in conjunction with Akay (1980) type successive iteration within each step. To treat nonlinear terms efficiently during the iteration, an iterative scheme with a constant coefficient matrix is employed. The ply damage region of the laminated shell is estimated using the Tsai-Wu criteria.

Numerical results, including the contact force history, deflection and strain of shell are obtained. The results of nonlinear analysis for the different radii of curvature are compared with the linear analysis results, which enables us to recognize when the small deflection theory may become inadequate and the large deflection theory should be used to give more accurate numerical estimation. The effect of the radii of curvature on the composite shell behaviors is also investigated and discussed.

2. Geometrical Nonlinear Formulation of Composite Shell

Consider a thin laminated composite cylindrical shell that is made of homogeneous orthotropic layers. An orthogonal curvilinear coordinate system (x, θ, z) is taken along the middle surface of the shell such that the x-axis is along the longitudinal axis of cylindrical shell, the θ-axis is in the hoop direction and z-axis perpendicular to the middle surface (Fig. 1). The cylindrical shell has a radius of curvature R and a total thickness h. In the extended Sander's shell theory (Rajagopalan, 1993), displacement components (u, v, w) which include transverse shear deformation at a point

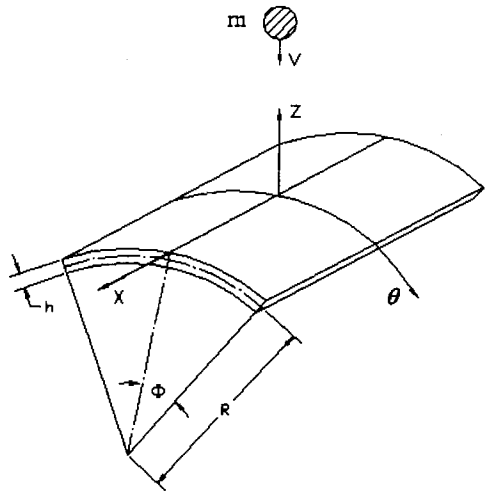

Fig. 1 Geometry of the composite cylindrical shell

(x, θ, z) of the shell are given by

$$\begin{aligned} u(x, \theta, z, t) &= u_0(x, \theta, t) + z\phi_x(x, \theta, t) \\ v(x, \theta, z, t) &= v_0(x, \theta, t)(1 + z/R) \\ &\quad + z\phi_\theta(x, \theta, t) \\ w(x, \theta, z, t) &= w_0(x, \theta, t) \end{aligned} \tag{1}$$

where u_0, v_0, and w_0 are the mid-surface displacements corresponding to the x, θ, and z directions, respectively; ϕ_x and ϕ_θ are independent rotations of the cross-sections about the θ and x axes respectively; and R is the radius of the cylindrical shell.

Using the von Karman large deflection assumptions (Reddy, 1997), the strain components can be expressed by

$$\{\varepsilon\} = \begin{Bmatrix} \varepsilon_x \\ \varepsilon_\theta \\ \gamma_{x\theta} \\ \gamma_{\theta z} \\ \gamma_{xz} \end{Bmatrix} = \begin{Bmatrix} \varepsilon_p \\ 0 \end{Bmatrix} + \begin{Bmatrix} z\varepsilon_b \\ \varepsilon_s \end{Bmatrix} + \begin{Bmatrix} \varepsilon_L \\ 0 \end{Bmatrix} \tag{2}$$

where

$$\{\varepsilon_p\} = \begin{Bmatrix} \dfrac{\partial u_0}{\partial x} \\ \dfrac{\partial v_0}{\partial \theta} + \dfrac{w}{R} \\ \dfrac{\partial u_0}{\partial \theta} + \dfrac{\partial v_0}{\partial x} \end{Bmatrix} \tag{3}$$

$$\{\varepsilon_b\}=\begin{Bmatrix} \dfrac{\partial \phi_x}{\partial x} \\ \dfrac{\partial \phi_\theta}{\partial \theta} \\ \dfrac{\partial \phi_x}{\partial \theta}+\dfrac{\partial \phi_\theta}{\partial x}+\dfrac{1}{2}\left[\dfrac{\partial v_0}{\partial x}-\dfrac{\partial u_0}{\partial \theta}\right] \end{Bmatrix} \tag{4}$$

$$\{\varepsilon_s\}=\begin{Bmatrix} \dfrac{\partial w}{\partial \theta}+\phi_\theta-\dfrac{v_0}{R} \\ \dfrac{\partial w}{\partial x}+\phi_x \end{Bmatrix} \tag{5}$$

and

$$\{\varepsilon_L\}=\begin{Bmatrix} \dfrac{1}{2}\left[\dfrac{\partial w}{\partial x}\right]^2 \\ \dfrac{1}{2}\left[\dfrac{\partial w}{\partial \theta}\right]^2 \\ \dfrac{\partial w}{\partial x}\dfrac{\partial w}{\partial \theta} \end{Bmatrix} \tag{6}$$

are the in-plane strains, bending strains, transverse shear strains and nonlinear parts of the in-plane strains, respectively.

Integration of the stresses (N, Q) and the stresses multiplied by z across the thickness of the cylindrical shell (M) results in the constitutive equation for a laminated shell (Zhao, 2000)

$$\begin{Bmatrix} N \\ M \\ Q \end{Bmatrix}=\begin{bmatrix} A & B & 0 \\ B & D & 0 \\ 0 & 0 & H \end{bmatrix}\left[\begin{Bmatrix} \varepsilon_p \\ \varepsilon_b \\ \varepsilon_s \end{Bmatrix}+\begin{Bmatrix} \varepsilon_L \\ 0 \\ 0 \end{Bmatrix}\right] \tag{7}$$

or symbolically,

$$\{\sigma\}=[\bar{D}](\{\varepsilon_0\}+\{\varepsilon_L\})=[\bar{D}]\{\varepsilon\} \tag{8}$$

In Eqs. (7) and (8), N_i, M_i and Q_i are the so called in-plane stress resultants, stress moments, and transverse shear forces, respectively. The coefficients A_{ij}, B_{ij}, D_{ij} and H_{ij} are the respective in-plane, bending-in-plane, bending and thickness shear stiffness; $\{\varepsilon_0\}$ and $\{\varepsilon_L\}$ are the generalized linear and nonlinear strains, respectively.

We shall consider a system consisting of a cylindrical shell and an impactor and applying the principle of virtual work to the system at time $t+\Delta t$ to then develop the finite element equations:

$$\int_{A_0}\{\delta u\}^{\mathrm{T}}[\rho]\{\ddot{u}\}dA+\int_{A_0}\{\delta\varepsilon\}^{\mathrm{T}}\{\sigma\}dA + \delta w_i m_i \ddot{w}_i+F\delta\alpha=0 \tag{9}$$

where A_0 is the original shell area; $[\rho]$ is the laminated cylindrical shell mass matrix; δ means the variation; $\{u\}$ is the generalized displacements defined in Eq. (10)

$$\{u\}=\begin{Bmatrix} u_0+z\phi_x \\ (1+\dfrac{z}{R})\,v_0+z\phi_\theta \\ w_0 \end{Bmatrix} \tag{10}$$

; m_i, w_i, and $\ddot{w}_i$ are the mass, displacement, and acceleration of the impactor, respectively.

F is the contact force between the shell and impactor; and α is the indentation given by

$$\alpha=w_i(t+\Delta t)-w_s(x_0,\ \theta_0,\ t+\Delta t) \tag{11}$$

in which w_s is the shell deflection at the impact point $(x_0,\ \theta_0)$.

3. Finite Element Formulation

The Finite element type used here is a nine-node iso-parametric quadrilateral element. Shell displacements in the element are interpolated by

$$\{u\}=\sum_{i=1}^{n}N_i[I]\{\Delta_i\} \tag{12}$$

where N_i are shape functions; $\{\Delta_i\}^{\mathrm{T}}=[u_{0i},\ v_{0i},\ w_{0i},\ \phi_{xi},\ \phi_{\theta i}]$ is the nodal displacement vector; and n is the number of nodes per an element. Substitution of Eq. (12) into Eq. (2) gives generalized strains $\{\varepsilon\}$ and their variations $\{\delta\varepsilon\}$:

$$\{\varepsilon\}=([B_0]+\frac{1}{2}[B_L])\{\Delta\} \tag{13}$$
$$\{\delta\varepsilon\}=([B_0]+[B_L])\{\delta\Delta\}$$

where $[B_o]$ and $[B_L]$ are the linear and nonlinear strain transformation matrices, respectively (see appendix for definitions). We shall note the matrix $[B_L]$ depends linearly on the vector $\{\Delta\}$. Substituting Eqs. (10) and (13) into Eq. (9) with $\{\delta\Delta\}$ and δw_i arbitrary, Eq. (9) can be partitioned into two sets of equations

$$m_i\ddot{w}_i+F=0 \tag{14}$$
$$[M]\{\ddot{\Delta}\}+[K_0]\{\Delta\}+[K_L(\Delta)]\{\Delta\}=\{F\} \tag{15}$$

where $[M]$ is the mass matrix of the laminated cylindrical shell, $[K_0]$ the linear stiffness matrix, $\{F\}$ contact force vector, and $[K_L(\Delta)]$ the generalized, unsymmetrical, nonlinear stiffness matrix given by

$$[K_L(\Delta)]=\int_{A_0}(\frac{1}{2}[B_0]^T[\bar{D}]\ [B_L]+[B_L]^T[\bar{D}]\ [B_0]+\frac{1}{2}[B_L]^T[\bar{D}]\ [B_L])\,dA \tag{16}$$

For the numerical evaluation of the stiffness matrix in Eq. (15) without shear locking, selective reduced integration method is employed. The 3×3 Gaussian rule is used to compute the stiffness coefficients for the in-plane and bending deformation while the reduced 2×2 rule is used to evaluate the terms associated with transverse shear deformation.

The shell and impactor motion is analyzed using Eqs. (14) and (15) with the contact force vector $\{F\}$ updated.

4. Contact Force

The contact force between the impactor and the cylindrical shell is considered to be a point load in the analysis. Upon loading the contact force is determined by applying the modified version of the Herzian contact law (Tan and Sun, 1985). The contact force F is related to indentation depth α by

$$F=\chi\alpha^{1.5} \tag{17}$$

where χ is the modified constant of the Hertz contact theory (Willis, 1966; Yang and Sun, 1982). For the indentor of 1.27cm diameter, the contact coefficient χ is found to be 1.413×10^6 N/cm$^{1.5}$. Upon unloading and re-loading the contact force is determined by (Crook, 1952; Yang and Sun, 1982)

$$F=F_m[(\alpha-\alpha_0)/(\alpha_m-\alpha_0)]^q \tag{18}$$

where q is a constant power: during unloading and re-loading q is 2.5 and 1.5, respectively; F_m is the maximum contact force just before unloading; α_m is the indentation corresponding to F_m; and α_0 is the permanent indentation during this loading-unloading process. The permanent indentation α_0 is determined from the following expressions

$$\alpha_0=\begin{cases}0 & \alpha_m<\alpha_{cr}\\ \beta(\alpha_m-\alpha_{cr}) & \alpha_m\geq\alpha_{cr}\end{cases} \tag{19}$$

where the coefficient β and the critical indentation α_{cr} are approximately 0.094 and 1.667×10^{-2} cm, respectively, for graphite/epoxy composites.

5. Solution Algorithm

In order to efficiently solve the nonlinear dynamics of Eq. (15), an iterative scheme with a constant coefficient matrix proposed by Akay is employed. Akay (1980) demonstrated both the efficiency and accuracy of the proposed algorithm. Chen and Sun (1985) also employed this scheme in studying the nonlinear transient behavior of composite laminates. In their studies, accurate results could be obtained with relatively coarse meshes and large time increments, although the Newmark's scheme would lose its unconditional stability.

In Akay's scheme, the nonlinear matrix $[K_L(\Delta)]$ in Eq. (15) is moved to the right-hand side of the equation and considered as a given "force" vector which depends upon the displacements computed in the previous iteration within each time step. The Nemark constant acceleration method is used for solving the time-dependent equations. Using this scheme, Eq. (15) can be expressed in iterative form at each time step by

$$[\bar{K}]\{\Delta\}^{i+1}_{t+\Delta t}=\frac{\Delta t^2}{4}\{F\}^i_{t+\Delta t}+[M]\{b\}_t-\frac{\Delta t^2}{4}[K_L(\Delta)]^i_{t+\Delta t} \tag{20}$$

where

$$[\bar{K}]=\frac{\Delta t^2}{4}[K_0]+[M]$$

$$\{b\}_t=\{\Delta\}_t+\Delta t\{\dot{\Delta}\}_t+\frac{\Delta t^2}{4}\{\ddot{\Delta}\}_t$$

In Eq. (20), i is the number of iterations within a time step. Successive iterations have to continue until a solution of the desired accuracy is reached in each time step. During the iteration process, the modified load vector on the right-hand side of Eq. (20) must be updated. On the other hand, the decomposition of the coefficient matrix needs to be done only at the initial time step. The same solution scheme is used for solving the equation for the motion of the impactor, i. e. Eq. (14). In

addition, the contact force has to be computed before the next iteration is carried out. Therefore, Eqs. (14) and (20) must be solved simultaneously with Eqs. (11) as well as (17) and (18).

6. Failure Criterion

Ply stresses are calculated and the shell is examined for failure in each node of elements using the Tsai-Wu failure criteria. In the Tsai-Wu general quadratic interaction criteria the failure surface in the stress space is described by tensor polynomial. Failure (Gibson, 1994) is assumed when

$$F_1\sigma_1+F_2\sigma_2+F_{11}\sigma_1^2+F_{22}\sigma_2^2+F_{66}\sigma_6^2 +2F_{12}\sigma_1\sigma_1\geq 1 \tag{21}$$

where σ_1, σ_2, and σ_6 are normal and shear stress components along principal material axes. The following strength parameters account for the lamina failure

$$\begin{aligned} F_{11}&=\frac{1}{X^+X^-}\\ F_1&=\frac{1}{X^+}-\frac{1}{X^-}\\ F_{22}&=\frac{1}{Y^+Y^-}\\ F_2&=\frac{1}{Y^+}-\frac{1}{Y^-}\\ F_{66}&=\frac{1}{S^2}\\ F_{12}&=-\frac{0.5}{\sqrt{X^+X^-Y^+Y^-}} \end{aligned} \tag{22}$$

where X^+ and X^- are the longitudinal tensile and compressive strengths of lamina; Y^+ and Y^- are the transverse strengths of lamina; and S is the in-plane shear strength.

The terms on the left-hand side of Eq. (20) are regarded as a failure index. The failure is assumed to occur when the stress states of some point are estimated to exceed the allowable value. On the other words, failure occurs if the failure index of the point is ≥ 1.

7. Numerical Results and Discussion

The formulation of the shell element discussed in the previous section has been implemented into a nonlinear finite element program. This program was utilized to analyze the problems; and the results are discussed as follows.

The composite cylindrical shell in the problems has the dimensions of $15.24\times 10.16\times 0.269$ cm. The shell is made of graphite/epoxy laminated with a stacking sequence of $[0°/45°/0°/-45°/0°]_{2s}$. The target shell is hinge supported and immovable along the four edges. Three different radii of curvature R, i. e., 10 cm, 20 cm and 50 cm are considered in the analysis. The cylindrical shell is assumed to be impacted perpendicularly at the center by a steel impactor with a mass of 8.53×10^{-3} Ns^2/m and a contacting spherical cap within a diameter of 12.7 mm. The impact velocity is set at 30m/s. From symmetry a quarter of the shell is modeled by a 4×4 mesh. The material properties and strengths are listed in Table 1.

The validity of the impact response of a cylindrical shell is first checked by comparing the contact force induced during impact with those for a plate. This was done by letting the radius of curvature of the cylindrical shell be very large (say 10^{15} cm) for a plate. Figure 2 shows the comparison of the impact force histories obtained by using the large deformation for shell and plate (Chen and Sun, 1985). It is seen that there is good agreement between the two contact force histories.

The impact force histories for shells with different radii of curvature under the same impact condition are shown in Fig. 3. The results obtained using the linear small-deformation theory are also shown as dotted line for easy comparison. There is no significant difference for maximum impact force between the large (nonlinear)

Table 1 Elastic Properties of a Graphite/epoxy Lamina (Chen and Sun, 1985)

$E_1=120$ GPa	$E_2=7.9$GPa	$\nu_{12}=0.3$
$G_{12}=G_{23}=G_{13}=5.5$ GPa		
$\rho=1.58\times 10^{-5}$Ns^2/cm^4		
$X^+=1448$ (MPa)	$X^-=1448$ (MPa)	
$Y^+=44.8$ (MPa)	$Y^-=248$ (MPa)	
$S=62.1$ (MPa)		

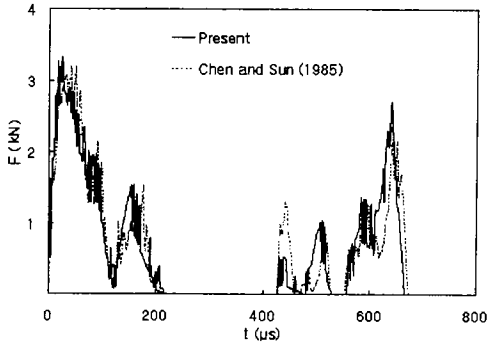

Fig. 2 Contact force histories of the present and Chen and Sun (1985)

and small (linear) deformation theories except for a shorter duration of impact for the nonlinear theory prediction. In Fig. 3 the linear and nonlinear theories predict four and five contacts, respectively, between the impactor and shell with $R=50$ cm. It is also found from Chen and Sun (1985) that two and four contacts are predicted by the linear and nonlinear theories, respectively, for the composite plate. There are two contacts predicted by the nonlinear theory during impact for the $R=20$ cm and $R=10$ cm shell, but a small third contact is still predicted by the linear theory for the $R=10$ cm shell. The reason is that shell modeled by the linear theory is more flexible than by the nonlinear theory. The total contact duration is longer for the flexible shell than for the stiff one. For the shells, when the radius of curvature is smaller, the separation between the impactor and shell after the first contact is shorter.

Figure 4 shows the relative motions of the cylindrical shell of $R=50$ cm and the impactor calculated by both linear and nonlinear theories. We shall note that the maximum deflection at the impact point is of the same order as the shell thickness using the linear small deformation theory, indicating that the large-deformation assumption has to be imposed. A reduction in the maximum deflection of the shell is predicted using the large-deformation theory. Figure 5 presents the effect of curvature on the deflection of the impact point. The maximum deflections are reduced with decreasing curvature, which stiffens

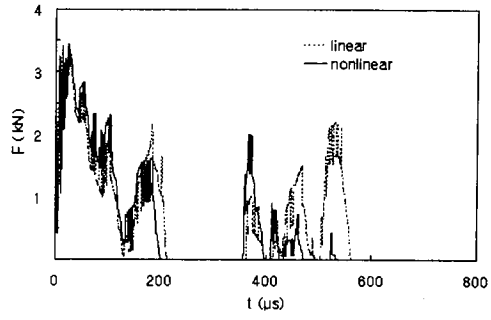

Fig. 3(a) Contact force histories, $R=50$cm

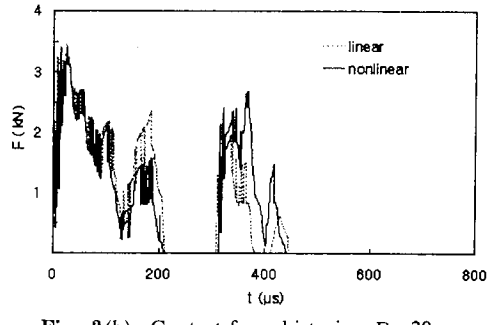

Fig. 3(b) Contact force histories, $R=20$cm

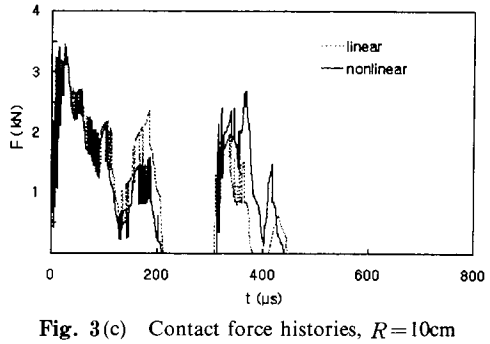

Fig. 3(c) Contact force histories, $R=10$cm

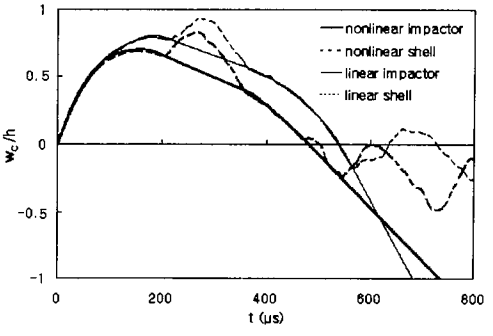

Fig. 4 Displacements of the impactor and shell ($R=50$cm)

the shell.

The calculated strain histories, ε_{xx}, for the shell $R=50$ cm at Gaussian point (0.215, 0.143 cm) on the surface opposite to the impacted surface are predicted in Fig. 6. The total strains and bending strains obtained by the linear theory do not greatly differ much. However the difference is observable by the nonlinear theory, in which the membrane strain yields significant action. Appar-

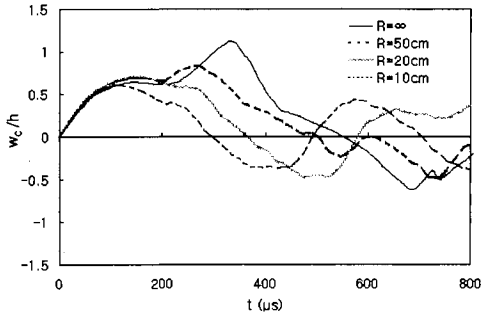

Fig. 5 Central deflection histories of the shells with different R

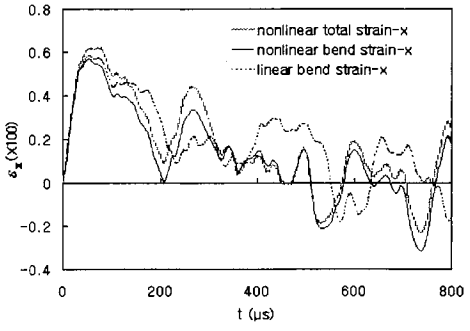

Fig. 6 Strain histories for the shell with $R=50$cm

Table 2 Maximum failure index in each layer of the shell (bold letters for predicted damage)

Ply	Maximum Failure Index							
	R=infinite		R=50 cm		R=20 cm		R=10 cm	
No.	linear	nonlinear	linear	nonlinear	linear	nonlinear	linear	nonlinear
1	**2.3367**	**2.1259**	**1.7608**	**1.393**	**1.0327**	0.9416	0.9808	0.8612
2	**1.9024**	**1.8607**	**1.3337**	0.9534	0.8984	0.8951	0.8505	0.8109
3	**1.7722**	**1.6022**	**1.2146**	0.7083	0.7712	0.7627	0.7223	0.7332
4	**1.372**	**1.0274**	0.9543	0.6725	0.707	0.5754	0.6087	0.6145
5	**1.0166**	0.9937	0.6692	0.6078	0.6097	0.5106	0.5552	0.573
6	0.8925	0.8982	0.5247	0.5866	0.4541	0.3507	0.5308	0.5046
7	0.6921	0.8407	0.4607	0.4452	0.2849	0.2755	0.2016	0.395
8	0.5736	0.673	0.3698	0.3419	0.1635	0.2137	0.1258	0.3326
9	0.3154	0.5679	0.1332	0.2973	0.1289	0.2044	0.1089	0.2137
10	0.179	0.4789	0.2521	0.2209	0.1001	0.2369	0.1193	0.2008
11	0.1669	0.4077	0.1393	0.2147	0.1429	0.2488	0.122	0.2246
12	0.2537	0.3806	0.3817	0.2963	0.3448	0.3107	0.4549	0.3392
13	0.6634	0.4957	0.3946	0.4458	0.5447	0.6638	0.8488	0.6701
14	0.4466	0.4432	0.5939	0.5309	0.4911	0.6534	0.6102	0.5462
15	0.7132	0.6545	0.5406	0.617	0.726	0.7165	0.9762	0.8769
16	0.8194	0.7196	0.7759	0.6223	0.8063	0.7938	**1.0773**	0.9381
17	0.6205	0.6674	0.8557	0.5236	0.6511	0.7426	0.8897	0.8321
18	0.9959	0.9435	0.933	0.8348	**1.2308**	**1.0043**	**1.4244**	**1.0117**
19	0.6597	0.7658	0.8771	0.7946	0.9834	0.9769	**1.0238**	0.928
20	**1.1237**	**1.0732**	**1.129**	0.993	**1.6992**	**1.4678**	**2.0701**	**1.8217**

ently, this difference is attributed to the nonlinear strain term $\{\varepsilon_L\}$.

Table 2 presents the maximum failure index in each ply of the shell with different radii of curvature. It is seen that the maximum failure index calculated by the nonlinear theory is smaller than by linear analysis. This means that stresses in the shell are reduced by nonlinear analysis compared with the linear analysis. Another interesting phenomenon is that the distribution of the maximum failure index according to the larger deformation theory is more uniform than the small deformation theory.

8. Conclusion

In this study, the impact response and damage behaviors are analyzed by using the nonlinear large-deformation theory for a laminated composite cylindrical shell under low velocity impact. From this the following is deduced.

① There is no significant difference for maximum contact force between the large and small deformation theories except for a shorter duration of impact for the nonlinear theory prediction. Linear theory always predicts longer contact time between the impactor and the shell. The reason is that the shell modeled by the linear theory is more flexible than by the nonlinear theory. The total contact duration is longer for flexible shells than for stiff ones. For the shells, when the radius of curvature is smaller, the separation between the impactor and shell after the first contact is shorter.

② The maximum strains and deflections do not occur at the same time. The large deformation theory predicts smaller deflection and bending strain; however, the total strain (bending plus membrane strain) is larger than that in the linear case, in which the membrane strain yields significant action.

③ The ply of the maximum failure index is different for the infinite and finite curvature laminates. The maximum failure index occurs at the bottom surface of the laminated plate but at the top for the laminated shell.

④ The maximum failure index calculated by the nonlinear theory is smaller than by linear analysis. This means that the stresses in the shell are reduced by nonlinear analysis comparing with the linear analysis. Distribution of the maximum failure index according to the large deformation theory is more uniform than the small deformation theory.

⑤ Maximum impact response in a laminated composite shell increases rapidly with the increase of the impact load. When the maximum deflection at the impact point is of the same order as the shell thickness, the nonlinear analysis is necessary. Otherwise, if small deformation theory is used, it will lead to significant error in the design of composite shells.

Acknowledgement

This work was supported by 1998 Inha University Research Fund.

References

Aggour, H. and Sun, C. T., 1988, "Finite Element Analysis of a Laminated Composite Plate Subjected to Circularly Distributed Central Impact Loading," *Computers & Structures*, Vol. 28, No. 6, pp. 729~736.

Akay, H. U., 1980, "Dynamic Large Deflection Analysis of Plates Using Mixed Finite Elements," *Computers & Structures*, Vol. 11, pp. 1~11.

Bachrach, W. E. and Hansen, R. S., 1988, "Mixed Finite-Element Method for Composite Cylinder Subjected to Impact," *AIAA J.*, Vol. 27, No. 5, pp. 632~638.

Chen, J. K. and Sun, C. T., 1985, "Dynamic Large Deflection Response of Composite Laminates Subjected to Impact," *Composite Structures*, Vol. 4, pp. 59~73.

Cho, C. and Zhao, G., 1999, "Dynamic Response and Damage of Composite Shell under Impact," *KSME Int. J.*, Vol. 13, No. 9, pp. 596~608.

Choi, I. H. and Hong, C. S., 1994, "New Approach for Simple Prediction of Impact Force History on Composite Laminates," *AIAA J.*, Vol. 32, No. 10, pp. 2067~2072.

Crook, A. W., 1952, "A Study of Some Impacts Between Metal Bodies by a Piezoelectric Method," Proceedings of the Royal Society, London, Series A, Vol. 212, p. 377.

Gibson, R. F., 1994, *Principles of Composite Material Mechanics*, McGraw Hill, pp. 110 ~111.

Gong, S. W., Toh, S. L. and Shim, V. P. W., 1994, "The Elastic Response of Orthotropic Laminated Cylindrical Shells to Low-Velocity Impact," *Composite Engineering*, Vol. 4, No. 2, pp. 247~266.

Matemilola, S. A. and Stronge, W. J., 1997, "Impact Response of Composite Cylinders," *Int. J. of Solids and Structures*, Vol. 34, pp. 2669 ~2684.

Rajagopalan, K., 1993, *Finite Element Buckling Analysis of Stiffened Cylindrical Shells*, A. A. Balkema (Rotterdam), pp. 27~28.

Reddy, J. N., 1997, *Mechanics of Laminated Composite Plates: Theory and Analysis*, CRC Press Inc., pp. 141~142.

Shivakumar, K. N., Elber, W. and Illg, W., 1985, "Prediction of Impact Force and Duration Due to Low-Velocity Impact on Circular Composite Laminates," *J. Applied Mechanics*, Vol. 52, pp. 674~680.

Tan, T. M. and Sun, C. T., 1985, "Use of Statical Indentation Law in the Impact Analysis of Laminated Composite Plate," *J. Applied Mechanics*, Vol. 52, pp. 6~12.

Willis, J. R., 1966, "Hertzian Contact of Anisotropic Bodies," *Journal of Mechanics and Physics of Solids*, Vol. 14, pp. 163~176.

Wu, E. B. and Yen, C. S., 1994, "The Contact Behavior Between Laminated Composite Plates and Rigid Spheres," *J. Applied Mechanics*, Vol. 61, pp. 60~66.

Yang, S. H. and Sun, C. T., 1982, "Indentation Law for Composite Laminates," *Composite Materials: Testing and Design, ASTM STP 787, ASTM*, pp. 425~449.

Zhao, G., 2000, *Impact Response and Post-buckling Behavior of Composite Cylindrical Shell*, Ph. D Thesis, Inha University, pp. 11~18.

Appendix

$$[B_0]=\left[[B^p]\ [B^b]\ [B^s]\right]^T \tag{A1}$$

$$[B_L]=\left[[B_L]\ [0]\ [0]\right]^T \tag{A2}$$

where $[B^p]$ is the in-plane strain-displacement transformation matrix,

$$[B_i^p]=\begin{bmatrix} \frac{\partial N_i}{\partial x} & 0 & 0 & & \\ 0 & \frac{\partial N_i}{\partial \theta} & \frac{N_i}{R} & 0 & 0 \\ \frac{\partial N_i}{\partial \theta} & \frac{\partial N_i}{\partial x} & 0 & & \end{bmatrix} \quad (i=1\sim 9) \tag{A3a}$$

$[B^b]$ is bending strain-displacement transformation matrix,

$$[B_i^b]=\begin{bmatrix} 0 & 0 & 0 & \frac{\partial N_i}{\partial x} & 0 \\ 0 & 0 & 0 & 0 & \frac{\partial N_i}{\partial \theta} \\ \frac{1}{2}\frac{\partial N_i}{\partial \theta} & \frac{1}{2}\frac{\partial N_i}{\partial x} & 0 & \frac{\partial N_i}{\partial \theta} & \frac{\partial N_i}{\partial x} \end{bmatrix} \quad (i=1\sim 9) \tag{A3b}$$

$[B^s]$ is the shear deformation strain-displacement transformation matrix,

$$[B_i^s]=\begin{bmatrix} 0 & -\frac{N_i}{R} & \frac{\partial N_i}{\partial \theta} & 0 & N_i \\ 0 & 0 & \frac{\partial N_i}{\partial x} & N_i & 0 \end{bmatrix} \quad (i=1\sim 9) \tag{A3c}$$

and $[B^L]$ is large deformation strain-displacement transformation matrix.

$$[B_i^L]=\begin{bmatrix} 0\ 0 & \frac{\partial w}{\partial x}\frac{\partial N_i}{\partial x} & 0\ 0 \\ 0\ 0 & \frac{\partial w}{\partial \theta}\frac{\partial N_i}{\partial \theta} & 0\ 0 \\ 0\ 0\ \frac{\partial w}{\partial \theta}\frac{\partial N_i}{\partial x}+\frac{\partial w}{\partial x}\frac{\partial N_i}{\partial \theta} & & 0\ 0 \end{bmatrix} \quad (i=1\sim 9) \tag{A4}$$